IJC
International Journal of Cancer

Long isoform of VEGF stimulates cell migration of breast cancer by filopodia formation via NRP1/ARHGAP17/Cdc42 regulatory network

Marina Kiso[1], Sunao Tanaka[1], Shigehira Saji[2], Masakazu Toi[1] and Fumiaki Sato[1]

[1]Department of Breast Surgery, Graduate School of Medicine, Kyoto University, Kyoto, Japan
[2]Department of Medical Oncology, Fukushima Medical University, Fukushima, Japan

VEGF stimulates endothelial cells as a key molecule in angiogenesis. VEGF also works as a multifunction molecule, which targets a variety of cell members in the tumor microenvironment. We aimed to reveal VEGF-related molecular mechanisms on breast cancer cells. VEGF-knocked-out MDA-MB-231 cells ($231^{VEGFKOex3}$) showed rounded morphology and shorter perimeter (1.6-fold, $p < 0.0001$). The $231^{VEGFKOex3}$ cells also showed impaired cell migration (2.6-fold, $p = 0.002$). Bevacizumab treatment did not induce any change in morphology and mobility. Soluble neuropilin-1 overexpressing MDA-MB-231 cells (231^{sNRP1}) exhibited rounded morphology and shorter perimeter (1.3-fold, $p < 0.0001$). The 231^{sNRP1} cells also showed impaired cell migration (1.7-fold, $p = 0.003$). These changes were similar to that of $231^{VEGFKOex3}$ cells. As MDA-MB-231 cells express almost no VEGFR, these results indicate that the interaction between NRP1 and long isoform of VEGF containing a NRP-binding domain regulates the morphology and migration ability of MDA-MB-231 cells. Genome-wide gene expression profiling identified *ARHGAP17* as one of the target genes in the downstream of the VEGF/NRP1 signal. We also show that VEGF/NRP1 signal controls filopodia formation of the cells by modulating Cdc42 activity via ARHGAP17. Among 1,980 breast cancer cases from a public database, the ratio of *VEGF* and *SEMA3A* in primary tumors (n = 450) of hormone-receptor-negative breast cancer is associated with *ARHGAP17* expression inversely, and with disease free survival. Altogether, the bevacizumab-independent VEGF/NRP1/ARHGAP17/Cdc42 regulatory network plays important roles in malignant behavior of breast cancer.

Key words: breast cancer, VEGF, neuropilin, ARHGAP17, filopodia, migration, cdc42, isoform

Abbreviations: BC: breast cancer; DFS: disease free survival; ECOG: Eastern Cooperative Oncology Group; ER: estrogen receptor; HR: hormone receptor; NRP1: neuropilin1; OS: overall survival; PFS: progression-free survival; SEMA3A: Semaphorin3A; sNRP1: soluble neuropilin1; TNBCs: triple negative breast cancers

Additional Supporting Information may be found in the online version of this article.

Conflict of interest: The authors declare that they have no conflicts of interest.

Grant sponsor: This research was funded by Grants-in-Aid for Scientific Research (#24390301, #16H05400, and #15K10059), Japan Society for the Promotion of Science

DOI: 10.1002/ijc.31645

History: Received 9 Oct 2017; Accepted 24 May 2018; Online 4 July 2018

Correspondence to: Fumiaki Sato, Department of Breast Surgery, Graduate School of Medicine, Kyoto University, Kyoto, Japan; E-mail: fsatoh@kuhp.kyoto-u.ac.jp; Tel: +81-75-751-3660

Introduction

Breast cancer (BC) is one of the most common forms of cancer, with more than 1,300,000 new cases and 450,000 deaths each year worldwide.[1] BC is classified into several subtypes, such as the estrogen receptor (ER) positive (luminal) subtype, HER2-enriched subtypes and triple-negative (TN) subtypes. TN breast cancers (TNBCs) are highly metastatic tumors with poor prognosis.[2] Approximately 15% of BC patients develop distant metastasis, which is responsible for about 90% of BC-associated mortality.[3] Therefore, it is important to understand the mechanisms underlying BC metastasis. Metastasis is a complex process that includes tumor cell invasion/migration/motility, intravasation, survival in blood or lymphatic circulation (resistant to anoikis), extravasation and regrowth in new environments.[4] However, the critical molecular mechanisms underlying tumor metastasis remain unclear.

Angiogenesis plays important roles in tumor progression. VEGF (also known as VEGF-A), secreted by tumor and stromal cells, enhances angiogenesis in tumor microenvironment.[5] Newly formed vessels provide oxygen and nutrients to assist tumor growth. Clinically, VEGF expression in BC tumors has been reported to be associated with worse prognosis.[6] Bevacizumab, an antibody that neutralizes VEGF, suppresses tumor

What's new?

Vascular endothelial growth factor (VEGF) acts on endothelial cells to promote blood vessel formation and tumor growth. In breast cancer, VEGF expression is associated with poor prognosis, though its effects on breast cancer cells are not well understood. Here, the long isoform of VEGF (VEGF165) was found to generate a signal through the transmembrane protein neuropilin-1 (NRP1), without acting on VEGF receptors. ARHGAP17, a RhoGAP family protein that regulates Cdc42 activity and controls filopodia formation and cell migration ability, was identified as a VEGF165 signaling target. The VEGF/NRP1/ARHGAP17 network likely contributes to malignant cell behavior in hormone receptor-negative breast cancer.

angiogenesis by blocking the VEGF signals in endothelial cells. The Eastern Cooperative Oncology Group (ECOG) conducted a randomized trial (E2100 trial) for metastatic BC patients to compare treatment arms of paclitaxel plus bevacizumab and paclitaxel alone.[7] The bevacizumab-containing regimen resulted in a significantly improved progression-free survival (PFS) (11.8 *vs.* 5.9 months, hazard ratio: 0.60, $p < 0.001$), although it did not have a significant impact on overall survival (OS). Two other bevacizumab-related randomized trials for metastatic BC, the AVADO trial[8] and the RIBBON-1 trial,[9] confirmed the E2100's findings that bevacizumab prolonged PFS but not OS.

Several mechanisms of this acquired resistance have been proposed, such as angiogenesis by alternative pro-angiogenic pathways,[10–13] and recruitment of vascular progenitors[14] and modulators.[15,16] In addition, hypoxia induced by anti-angiogenic therapy promotes selection of aggressive cancer cells[17] and expansion of cancer stem cell pool.[18] According to recent studies, VEGF is a multifunction molecule targeting not only endothelial cells but also other cell members in the tumor microenvironment, including cancer cells, fibroblasts, immune cells and more.[5] However, VEGF's direct effect on cancer cells is not yet fully understood. Thus, we focused on the direct effect of VEGF on cancer cells, and hypothesized that there would be a VEGF-induced signal that contributes to the malignant behavior of BC cells.

In general, BC cells express almost no or very low level of VEGFR1/2. However, BC cells/tissues as well as other malignancies express various amounts of other VEGF receptors, neuropilins-1/2.[19–22] One neuropilin, NRP1, is a transmembrane protein that consists of a large extracellular domain, one transmembrane domain, and a relatively short cytoplasmic tail. The extracellular domains of NRP1 are divided into the a1–a2 subdomain, which binds semaphorins, the b1–b2 subdomain, which binds VEGF and supports semaphorin binding to the a1–a2 domain and the c domain, which mediates NRP dimerization.[23] Semaphorin3A (SEMA3A), which has recently been reported to be a tumor suppressor gene,[24] competitively binds to NRP1 to modulate VEGF–VEGFR–NRP1 interaction.[23]

In the present study, to investigate the direct effect of VEGF on BC cells, we generated VEGF knocked-out MDA-MB-231 cells (231^{VEGFKO} cells). Using these cells, we demonstrated that NRP1 signal by long isoform of VEGF (VEGF165), but not short isoform (VEGF121), regulates the morphology and migration ability of BC cells, and identified ARHGAP17, a rhoGAP, as a target gene of VEGF/NRP1 signaling. We also showed that VEGF/NRP1 signaling activates Cdc42 by suppressing ARHGAP17, and enhances filopodia formation and cell migration. Furthermore, using a publicly available dataset, we demonstrated that the VEGF/NRP1/ARHGAP17 regulatory network correlated with disease-free survival of hormone-receptor (HR)-negative BC patients.

Material and Methods

Detailed information regarding the material and methods used in this study is provided in the Supporting Information.

Cell culture and reagents

The cells and reagents used in this study are listed in Supporting Information.

CRISPR/Cas9 system and LentiCRISPRv2 infections

The CRISPR/Cas9 system was used to generate VEGF knockout MDA-MB-231 cells and Hs578T cells. The guide RNA (gRNA) sequences for knockdown of *VEGFA* were designed using a CRISPR gRNA Design Tool. The synthesized gRNA fragments were cloned into the *BsmB*I site of a lentiCRISPRv2 construct (Addgene, 52961), which contains a puromycin resistance marker. Viral particles containing gRNA for *VEGFA* and Cas9 were produced and transformed into MDA-MB-231 cells and Hs578T cells, according to the manufacturer's instructions.

Development of MDA-MB-231 cells overexpressing soluble NRP1 (sNRP1)

The lentivirus system (Life Technologies, K2400-20, Carlsbad, CA) was used to introduce sNRP1 into wild-type MDA-MB-231 cells. Stably infected cells were selected with Blasticidin (10 μg/mL) for 7 days.

Migration assay

BC cells were placed into each Transwell® chamber and migrating cells were counted using an inverted microscope (Keyence, BZ-9000).

Knockdown of genes by siRNA oligos

SiRNA oligo duplexes, GeneSolution siRNA, were purchased from Qiagen (Germany). Information on the siRNAs is listed in Supporting Information Table S9. Cells were treated with complex of siRNA oligos (0.1–0.2 μg/well) and X-tremeGENE siRNA Transfection Reagent (Roche Diagnositcs, Inc, Germany). Negative Control siRNAs (siControl, Qiagen) were used for mock transfection treatment.

Procedure to identify target genes of VEGF/NRP1 signal

To identify the target genes in the downstream of the VEGF/NRP1 signal network, we conducted genome-wide gene expression profiling of MDA-MB-231 cells (231^{WT}), $231^{VEGFKOex3}$ cells, and $231^{VEGFKOex3}$ cells exposed to human recombinant VEGF165 (rhVEGF165). Agilent SurePrint G3 Human GE 8 × 60 K Microarray (Agilent technologies) was used.

For the screening of differentially expressed genes, the microarray data was processed using Matlab software (R2016b, The Mathworks, Inc., MA).

G-LISA of Cdc42

To assess activation level of Cdc42, we used an ELISA-based assay, because G-LISA assay is more sensitive and quantitatively accurate than a GST–p21-activated kinase (PAK)–Cdc42-interactive binding domain pull-down assay as previously reported.[25] The cells were seeded and serum starved by serial incubations with 10% FBS for 72 hr, 0.5% FBS for 24 hr and then 0% FBS for 24 hr. Cdc42 activation level was measured using a G-LISA kit for Cdc42 (colorimetric format; Cytoskeleton, Denver, CO) according to the manufacturer's protocol. Developed color was scanned by a microplate reader (SPECTRAMAX340PC, Molecular Devices, CA).

ELISA for VEGF

VEGF concentration in culture media was analyzed using a colorimetric ELISA kit for human VEGF (Cat. No.RSD-DVE00-1, R&D Systems Inc.).

Scanning electron microscopy

The cells were seeded onto polyethylene terephthalate coverslips (Thermanox X™ disks, NUNC, Rochester, NY). The cells were serially fixed with 2% glutaraldehyde (Wako Pure Chemical Industries, Kyoto, Japan) at 4°C overnight, and then with 1% OsO_4 for 2 hr. The fixed cells were dehydrated, dried, and coated with a thin layer of platinum palladium. The specimens were then scanned using an S-4700 scanning electron microscope (Hitachi, Tokyo, Japan). Then, for each cell, the number of filopodia of 50 cells were counted using ImageJ software. Protrusions which were thinner than 0.37 μm and longer than 0.87 μm were counted as filopodia.

Cell proliferation assay

We performed cell proliferation assay in two ways; direct counting and WST-8 assay (Cell Counting Kit-8, Dojindo Molecular Technologies, Inc., Kumamoto).

Perimeter measurement

Photo images for each cell were taken using a KEYENCE BZ 9000 microscope and the perimeters of the cells were measured using ImageJ software.

Validation analysis using a public dataset

The dataset of the METABRIC study was obtained from the cBioportal website. This dataset contains demographic information, survival outcomes, subtyping, gene-expression data and genomic abnormality. All survival analyses were performed using Matlab software (version 2016b).

Western blotting

To analyze ARHGAP17 and NRP1 protein level, we performed immunoblotting with anti-ARHGAP17 antibody (LSBio, Anti-ARHGAP17/NADRIN Antibody (aa331–380) LS-C120326, Seattle, WA) and anti-NRP1 antibody (Cell Signaling Technology, Neuropilin-1 (D62C6) Rabbit mAb, Danver, MA). Rather than using secondary antibody to probe for primary antibody binding, the Easy-Western-II detection system (Beacle, BCL-EZS21, Kyoto, Japan) was employed. For an internal control, we used mouse anti-β-actin antibody (Abcam, ab6276, Cambridge, UK, 1/5,000 dilution), and goat anti-mouse IgG antibody conjugated to a peroxidase (Pierce biotechnology, 31340, Rockford, IL, 1/50,000 dilution). The chemical luminescence reagent used was ECL Select (GE Healthcare, Buckinghamshire, UK). Signals were detected by Ez-CaptureII (ATTO, Tokyo, Japan) with ImageSaver5 software (ATTO).

Results

Knockout of *VEGF* gene altered cell morphology, and decreased migration ability of MDA-MB-231 cells

VEGF is a multifunctional molecule which targets a variety of cell members in the tumor microenvironment. The aim of the current study was to investigate the direct effects of VEGF on BC cells. First, we used bevacizumab for a loss-of-function experiment. According to qRT-PCR analysis of VEGF using a BC cell line panel, TNBC cell lines expressed higher level of VEGF than luminal BC cell lines (Supporting Information Figs. S1a and S1*b*). Among TNBC cells, we chose MDA-MB-231 (wild-type: 231^{WT}) cells for the further experiments. A series of experiments showed that bevacizumab treatment did not induce any phenotypic change in cell proliferation (Fig. 1*a*), morphology (Figs. 2*a*, 2*c* and 2*h*) and migration (Fig. 2*i*) of 231^{WT} cells.

Next, we knocked out *VEGF* of 231^{WT} cells utilizing the CRISPR/Cas9 system to determine whether VEGF has direct effect on the phenotype of 231^{WT} cells or not. *VEGF* has several transcriptional variants that correspond to different sizes of VEGF molecules, such as VEGF121, VEGF165, VEGF189, VEGF206 and others (Fig. 1*b*). We designed a gRNA sequence of CRISPR/Cas9 system to target exon3 of *VEGF*, that is common in all variant VEGF forms. Then, *VEGF* knocked-out MDA-MB-231 cells ($231^{VEGFKOex3}$) were established by introducing the gRNA and Cas9 using a lentiviral system. Then, genomic sequences of VEGF exon3 in VEGFKO cells were checked by Sanger Sequencing (Supporting Information Fig. S2*a*). Among seven $231^{VEGFKOex3}$ clones checked, six

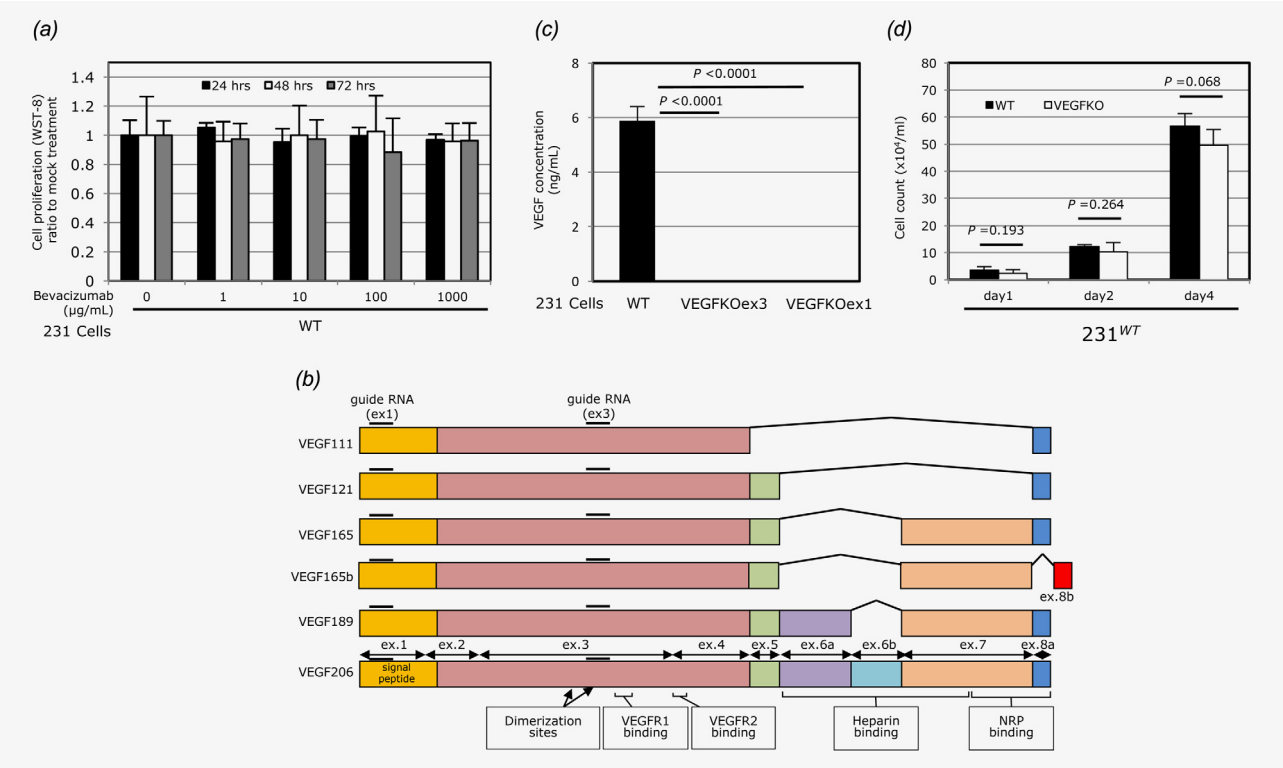

Figure 1. Knocking out of VEGF by CRISPR-Cas9 system. (*a*) Cell proliferation assay using WST-8. Bevacizumab treatment did not produce any significant changes in proliferation of MDA-MB-231 cells. (*b*) Schematic diagram depicting VEGF isoforms and the locations of guide RNA (gRNA) on the *VEGF* locus. The gRNA was placed on a common exon of all VEGF isoforms. (*c*) Protein expression levels of VEGF in culture media of 231^{WT} cells and 231^{VEGFKO} cells. VEGF was not detectable in culture media of the VEGFKO cells. (*d*) Cell growth rate by direct counting. There was not any significant difference in the cell growth rate between 231^{WT} cells and $231^{VEGFKOex3}$ cells. The doubling times of the 231^{WT} and $231^{VEGFKOex3}$ cells in the exponential phase (Day2–4) were almost identical at 21.7 and 21.2 hr, respectively. In *a, d* and *e*, bars and error bars: mean ± standard deviation of triplicated experiments. [Color figure can be viewed at wileyonlinelibrary.com]

clones had frame-shift mutations that generate truncated VEGF molecules without any of VEGFR1- (exon3), VEGFR2- (exon4), heparin- (exon6–7) or neuropilin- (exon7) binding domains (Fig. 1*b*).[26] In contrast, one clone had an in-frame mutation lacking only 12 amino acids. However, this deleted site overlapped with one of the dimerization sites (cysteine-notches) and a VEGFR1 binding site. This clone would not be functional. In addition, we confirmed by VEGF ELISA assay that the $231^{VEGFKOex3}$ cells did not actually secrete any detectable VEGF molecules (Fig. 1*c*).

Unlike the bevacizumab-treated 231^{WT} cells, the $231^{VEGFKOex3}$ cells exhibited different phenotypes in cell morphology and migration from 231^{WT} cells. The $231^{VEGFKOex3}$ cells had a small, rounded shape, whereas the 231^{WT} cells showed a larger and spindle-like shape (Figs. 2*a* and 2*b*). To quantify the morphological features, we measured the perimeters of the different cell types using Image-J software. The perimeter of the $231^{VEGFKOex3}$ cells was significantly shorter than that of the 231^{WT} cells (Fig. 2*h*, $p < 0.0001$). In addition, exposure of the $231^{VEGFKOex3}$ cells to exogenous rhVEGF165 restored their cell size, spindle-like shape (Fig. 2*d*), and perimeter to similar sizes, shapes and perimeter of those of the 231^{WT} cells (Fig. 2*h*).

Next, cell migration assay using Transwell® chambers demonstrated that the $231^{VEGFKOex3}$ cells had lower migration ability than the 231^{WT} cells (231^{WT} *vs.* $231^{VEGKOex3}$: $p = 0.002$), and that exposure to rhVEGF165 restored cell migration ability to an even higher level than the original level ($231^{VEGFKOex3}$ *vs.* $231^{VEGFKOex3}$ + rhVEGF165: $p = 0.0005$) (Fig. 2*i*). These results indicate that VEGF depletion caused the morphologic change, and suppressed cell migration in the 231^{WT} cells.

To eliminate the possibility of off-target effect of CRISPR-system, we also generated another VEGF knocked out 231 cell clone targeted at exon1 ($231^{VEGFKOex1}$). Then, genomic sequences of VEGF exon1 in $231^{VEGFKOex1}$ cells were checked by Sanger Sequencing (Supporting Information Fig. 2*b*). The $231^{VEGFKOex1}$ cells had mostly similar morphological and cell motility phenotype to $231^{VEGFKOex3}$ cells. The $231^{VEGFKOex1}$ showed shorter perimeter (231^{WT} *vs.* $231^{VEGFKOex1}$, $p < 0.0001$, Fig. 2*h*) and lower migration ability (231^{WT} *vs.* $231^{VEGFKOex1}$, $p = 0.0005$, Fig. 2*i*) compared to 231^{WT} cells.

These findings indicated that these morphological and cell motility phenotype is not due to off-target effect of CRISPR-system, but due to VEGF-depletion.

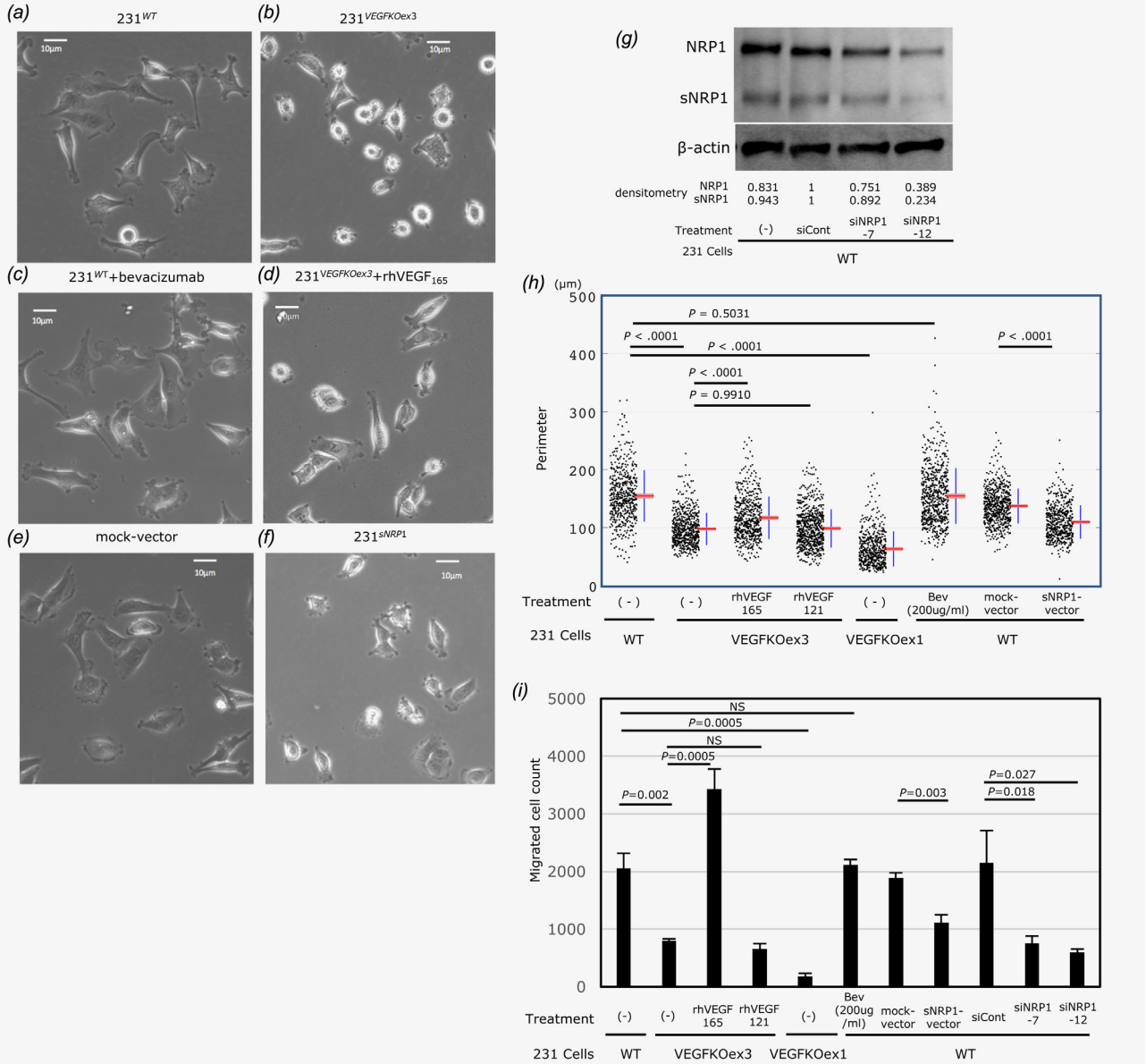

Figure 2. VEGF knock out induced morphologic change in MDA-MB-231 cells. Phase contrast microscope images of (*a*) wild type 231 cells (231^{WT}), (*b*) $231^{VEGFKOex3}$ cells, (*c*) bevacizumab-treated 231^{WT} cells, (*d*) rhVEGF165-treated $231^{VEGFKOex3}$ cells, (*e*) mock-vector-treated 231^{WT} cells, (*f*) 231^{sNRP1} cells. (*g*) Western blotting shows NRP1 expression was knocked down by siRNA. (*h*) Comparison of perimeter of these cells measured using ImageJ software. *p*: *p*-values of the Mann–Whitney *U* test. (*i*) Cell migration assay using Transwell chambers. Ten thousand cells were seeded into chambers. Twenty-four hours later, migrated cells in 10 random microscopic fields were counted. Bars and Error bars: mean ± standard deviation of triplicated experiments. In *h*–*i*, *p*: *p*-values of Student's *t*-test, NS: not significant. [Color figure can be viewed at wileyonlinelibrary.com]

On the other hand, the knocking out of VEGF did not affect the cell proliferation of the 231^{WT} cells (Fig. 1*d*). The doubling times of the 231^{WT} and $231^{VEGFKOex3}$ cells in the exponential phase (Day2–4) were almost identical at 21.7 and 21.2 hr, respectively. In summary, these data showed that knocking-out of VEGF induced rounded cell shape, and reduced cell migration, and indicated that VEGF could stimulate breast cancer cells directly.

Interaction between VEGF and NRP1 is responsible to phenotypic changes of 231^{VEGFKO} cells

As the findings of the bevacizumab treatment and *VEGF*-knockout experiments appeared to differ, we endeavored to explain the underlying molecular mechanisms of these discrepancies. Bevacizumab is an anti-VEGF antibody that binds to the VEGFR1/2-binding domain (exon3–4) of VEGF to inhibit the VEGF/VEGFR signaling pathway. However, NRP1

interacts with the exon7 portion of VEGF, which bevacizumab may be unable to block.[27] Moreover, mRNA expression of VEGFR1/2, and NRP2 in the BC cells were significantly lower than those in the endothelial cells (Supporting Information Figs. S1c, S1*d* and S1*g*), whereas mRNA expression of NRP1 in the BC cells was comparable to that in the endothelial cells (Supporting Information Figs. S1e and S1*f*). Therefore, we hypothesized that signaling produced by VEGF/NRP1 without VEGFR1/2 may contribute to the phenotypic changes of VEGF-knocked out cells.

To prove the hypothesis, we utilized a soluble form of neuropilin-1 (sNRP1), a naturally existing isoform of NRP1, which consists of the NRP1 extracellular domain with a VEGF-binding site. The sNRP1 works as a VEGF-trap to inhibit the VEGF–NRP1 interaction.[28] Then, sNRP1 was introduced into the MDA-MB-231 cells (231^{sNRP1} cells) by a lentivirus vector system. As expected, the 231^{sNRP1} cells showed smaller and more rounded morphology (Fig. 2*f*), with a significantly shorter perimeter than the control cells (Fig. 2*h*, 1.3-fold, $p < 0.0001$). In addition, the 231^{sNRP1} cells had lower migration ability than the control cells (Fig. 2*i*, 1.7-fold, $p = 0.003$). These findings demonstrated that the phenotypes of the 231^{sNRP1} cells were similar to those of the $231^{VEGFKOex3}$ cells, and indicate that interaction of VEGF and NRP1 contribute to phenotypic changes of cell morphology and motility. However, it remains unknown as to which of the following two scenarios are true: that the VEGF–NRP1 interaction directly produces a signal without VEGFR1/2; or that the interaction inhibits a signal produced by NRP1 and another NRP1-interacting molecule, such as SEMA3A. To determine whether VEGF–NRP1 interaction directly produces a signal or not, NRP1 expression was knocked down by siRNA (Fig. 2*g*, Supporting Information Fig. S3). The knock down efficiencies of siNRP1 was checked by RT-PCR blotting and western blotting. The knock down efficiencies of siNRP1–7 and siNRP1–12 were 54.2 and 58.9% in mRNA level, respectively (Supporting Information Fig. S3). The knock down efficiencies were 24.9 and 61.1% for protein level of membrane anchored NRP, and 10.8 and 76.6% for sNRP1, respectively (Fig. 2*g*). The NRP1-knocked down 231 (231^{NRP1KD}) cells exhibited lower cell migration ability than the 231^{WT} cells (Fig. 2*i*, 3.7-fold, $p = 0.017$). Assuming SEMA3A-NRP1 binding produce a signal to induce rounded cell shape and to reduce cell migration in $231^{VEGFKOex3}$ cells, 231^{sNRP1} cells and 231^{NRP1KD} cells would lose this SEMA3A-NRP1 signal and are supposed to make different cell morphology and mobility. However, actual morphologic and mobility phenotypes of $231^{VEGFKOex3}$ cells, 231^{sNRP1} cells and 231^{NRP1KD} cells displayed almost identical phenotypes. Thus, we concluded that VEGF–NRP1 binding but not SEMA3A-NRP1 binding produced a signal to regulate cell morphology and cell migration ability.

Taken together, these results indicated that cell signals produced by VEGF–NRP1 interaction may contribute to phenotypic changes of $231^{VEGFKOex3}$ cells.

Identification of genes in downstream of VEGF/NRP1 signal pathway

To identify genes in the downstream of VEGF/NRP1 signal network, we conducted a microarray-based gene expression analysis of 231^{WT} cells, $231^{VEGFKOex3}$ cells and $231^{VEGFKOex3}$ cells exposed to rhVEGF165. Genes in the downstream of the VEGF/NRP1 signals are supposed to be up/down-regulated in $231^{VEGFKOex3}$ cells, and rhVEGF165 treatment restores the expression to the 231^{WT} cell level. Among the filtered expression data of 16,052 coding genes (Supporting Information Table S1), 765 genes were more than twofold up/down-regulated in the $231^{VEGFKOex3}$ cells (Fig. 3*a*, Supporting Information Table S2), compared to 231^{WT} cells. Among these 765 genes, the expression levels of only 62 genes were restored by rhVEGF165 treatment (Fig. 3*b*). Thus, we chose these 62 genes as candidate genes (51 up-regulated and 11 down-regulated genes in $231^{VEGFKOex3}$ cells); they are listed in Supporting Information Table S3. To check whether this screening was properly executed, we performed gene ontology analysis using the DAVID tools.[29,30] A functional annotation chart (Supporting Information Table S4) showed that, despite the 3rd rank in total, term "cell migration" was listed in the highest rank as bioprocess category, which would be compatible with our findings that VEGF/NRP1 signal is associated with cell migration.

ARHGAP17 (also known as RICH1) was up-regulated 4.6-(=$2^{2.212}$) fold in the $231^{VEGFKOex3}$ cells (Fig. 3*c*, Supporting Information Table S3). Although ARHGAP17 is not defined as a cell migration-related gene in the DAVID files, it is a Rho-GAP that is known to interact with Cdc42[31] and to inactivate it, a member of the Rho family, regulating cell cytoskeleton organization and cell migration. ARHGAP17 expression was validated by a quantitative RT-PCR method. ARHGAP17 expression was significantly up-regulated in the $231^{VEGFKOex3}$ cells compared to the 231^{WT} cells (Fig. 4*a*, 1.74-fold, $p = 0.0036$), and was restored by rhVEGF165 treatment ($231^{VEGFKOex3}$ *vs.* $231V^{EGFKOex3}$ + rhVEGF165: 0.58-fold, $p = 0.003$). In addition, introduction of exogenous sNRP1 into the 231^{WT} cells up-regulated ARHGAP17 expression (1.79-fold, $p = 0.0029$). Western blotting also showed ARHGAP17 expression was significantly up-regulated in the $231^{VEGFKOex3}$ cells compared to the 231^{WT} cells by 2.14-fold (Fig. 4*b*).

The activity status of small GTPase molecules, including Cdc42, is regulated by GAPs, GEFs and GDIs. Among these 81 regulators, 11 ARHGAPs, 4 ARHGEFs and 2 GDIs are known to interact with Cdc42 (Supporting Information Table S5*a*). Among 17 Cdc42-regulators, only *ARHGAP17* meet selection criteria as VEGF-dependent genes (Fig. 3*c*, Supporting Information Fig. S4a). As demonstrated in previous reports, ARHGAP17 interacts with Cdc42 and regulates its activeness.[31] Similarly, the expression levels of 42 genes that are known to interact with NRP1 were also checked (Supporting Information Table S5*b*). However, knocking out VEGF did not alter the expression of any NRP1-interacting

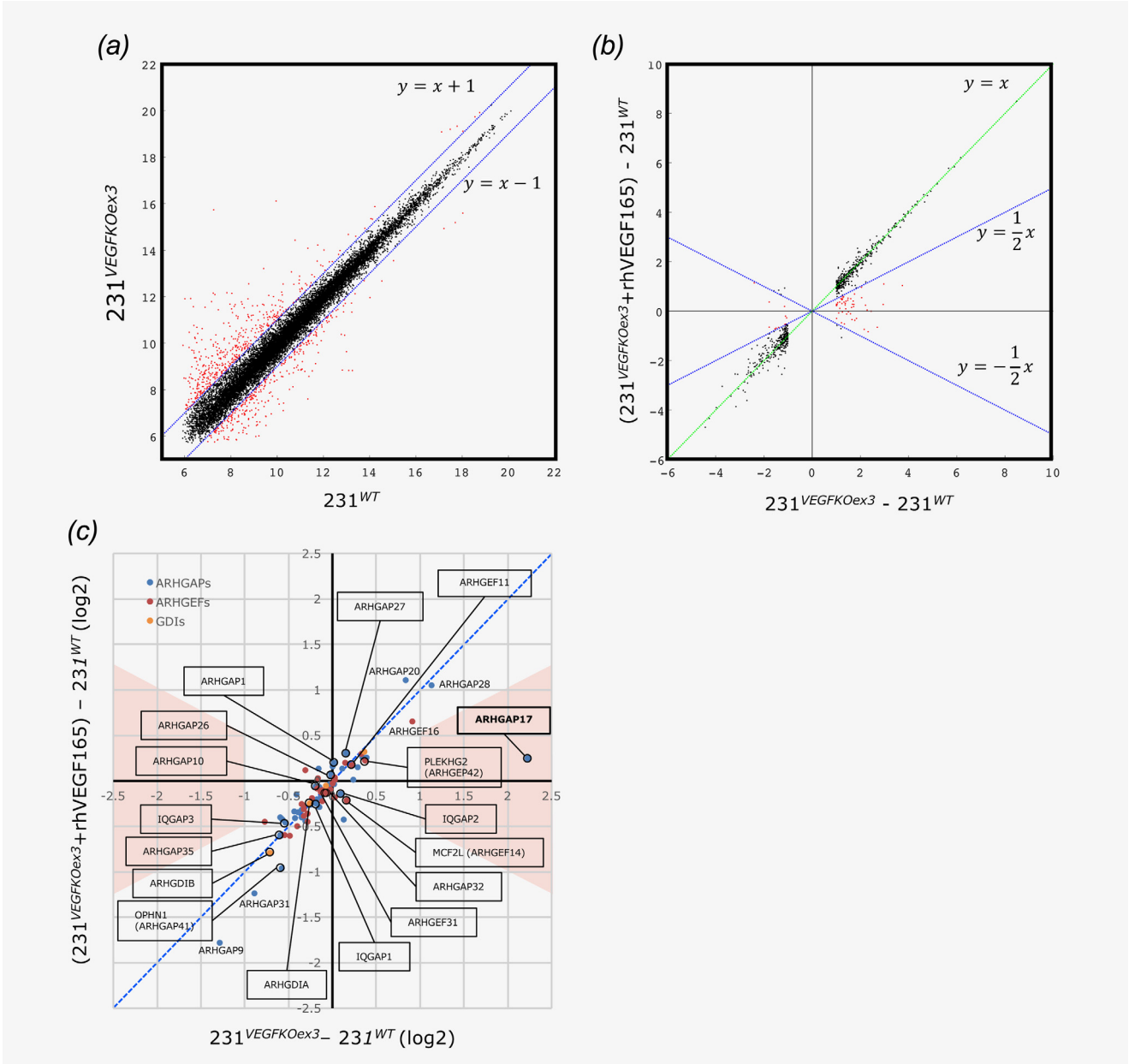

Figure 3. Whole-genome expression analysis to identify VEGF/NRP1-dependent genes. To identify genes in the downstream of the VEGF/NRP1 signal, we conducted genome-wide gene expression profiling of 231^{WT} cells, $231^{VEGFKOex3}$ cells and $231^{VEGFKOex3}$ cells exposed to rhVEGF165, using Agilent SurePrint G3 Human GE 8 × 60 K Microarray. Probe signal values of the genes were transformed into log2. (*a*) Scatter plot of 231^{WT} cells (x-axis) and $231^{VEGFKOex3}$ cells (y-axis). More than twofold up/down-regulated genes in $231^{VEGFKOex3}$ cells were shown as red dots (n = 765). (*b*) Scatter plot of 765 up/down-regulated genes. X-axis: $231^{VEGFKOex3}/231^{WT}$ ratio in log2, Y-axis: $(231^{VEGFKOex3}$ + rhVEGF165)/ 231^{WT} ratio in log2. Genes in which expression levels were restored 50 to 150% by rhVEGF165 treatment are shown as red dots (n = 62). (*c*) Fold-change between $231^{VEGFKOex3}$ and 231^{WT} cells, and recovery by rhVEGF165 treatment for *ARHGAPs*, *ARHGEFs* and *GDIs*. X-axis: fold change between $231^{VEGFKOex3}$ and 231^{WT} cells, Y-axis: fold change between $231^{VEGFKOex3}$ cells treated with rhVEGF165 and 231^{WT} cells. Blue dashed line: recovery rate equal to 0%. Dots in orange shade area: genes with more than twofold change and with recovery rate ranging from 50 to 150%. [Color figure can be viewed at wileyonlinelibrary.com]

genes (Supporting Information Figs. S4b and S4*c*). Taken together, these microarray analysis results identified ARHGAP17 as a top candidate gene working in the downstream of VEGF/NRP1 signal, and we focused upon ARHGAP17 in further analysis.

Regulation of Cdc42 by ARHGAP17 is responsible for VEGF/NRP1-dependent morphologic and mobility changes

Rho family members, such as RhoA, Rac1 and Cdc42, cycle between inactive GDP-bound form and active GTP-bound form. ARHGAPs (RhoGAPs) hydrolyze GTP bound to active-

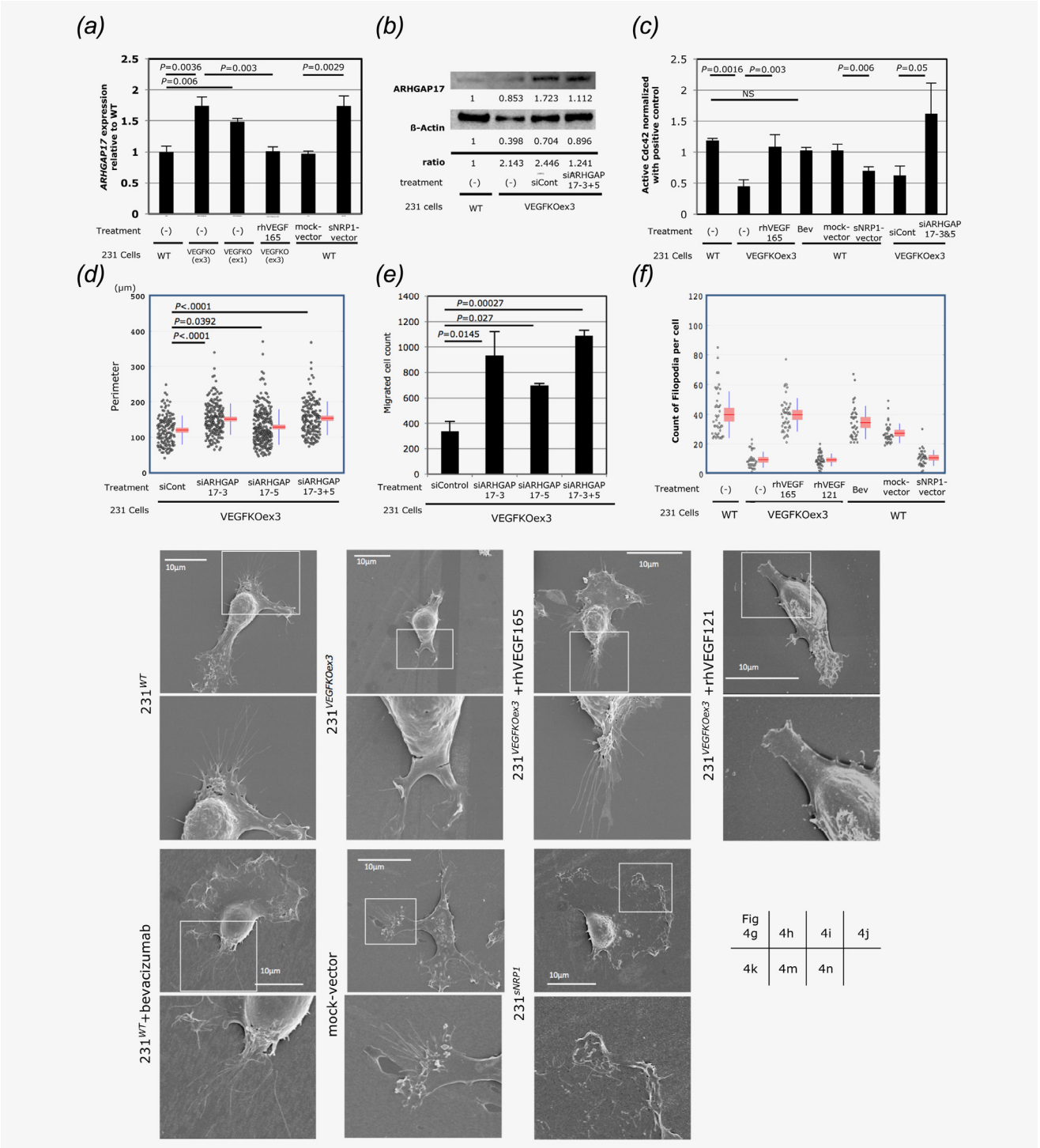

Figure 4. ARHGAP17 and Cdc42 status correlated with cell morphology and mobility. (*a*) mRNA expression of *ARHGAP*17 by qRT-PCR. (*b*) Western blotting shows ARHGAP17 was upregulated in $231^{VEGFKOex3}$ cells compared to 231^{WT} cells. It also shows ARHGAP17 expression was successfully knocked down by siRNA. (*c*) Quantitative measurement of active Cdc42 by G-LIZA assay. (*d*) Perimeters of siARHGAP17-treated cells, measured by Image-J. (*e*) Cell migration assay using Transwell chamber. (*f*) Count of filopodia per cell is shown. For each cell condition, the number of filopodia of 50 cells were counted. (*g*–*n*) Photos by scanning electron microscopy (*g*) 231^{WT} cells, (*h*) $231^{VEGFKOex3}$ cells and (*i*) rhVEGF165-treated $231^{VEGFKOex3}$ cells, (*j*) rhVEGF121-treated $231^{VEGFKOex3}$ cells, (*k*) bevacizumab treated MDA-MB-231 cells, (*n*) 231^{sNRP1} cells and (*m*) control cells. In *a, c,* and *e*, bars and error bars: mean ± standard deviation of triplicated experiments. In *a* and *c*–*e*, *p*: *p*-values of Student's *t*-test, NS: not significant. [Color figure can be viewed at wileyonlinelibrary.com]

form into GDP and phosphate to inactivate Rho family members, whereas ARHGEFs (RhoGEFs) exchange GDP bound to inactive-form with GTP to activate the Rho family members. ARHGAP17 acts as a Cdc42-selective RhoGAP, and it inactivates Cdc42.[31] As shown above, ARHGAP17 expression was regulated by VEGF/NRP1 signaling. Thus, to verify the relationship between VEGF/NRP1 signaling and Cdc42 status, we performed G-LISA assays on Cdc42 to measure and compare the amount of active Cdc42 in various cells as follows.

First, the association between ARHGAP17 and Cdc42 status was confirmed. In this analysis, we used two siRNAs to knock down ARHGAP17 of $231^{VEGFKOex3}$ cells. Introducing siRNAs against ARHGAP17 (Fig. 4*b*, Supporting Information Fig. S5) upregulated active Cdc42 level for more than twofold (Fig. 4*c*, 2.59-fold, $p = 0.05$), indicating that ARHGAP17 expression inversely correlated with Cdc42 status. Second, association between VEGF/NRP1 signaling and Cdc42 status was confirmed. The amounts of active Cdc42 were reduced only in the $231^{VEGFKOex3}$ cells and the 231^{sNRP1} cells in which the ARHGAP17 level was up-regulated (p-value = 0.0016 and 0.006, respectively). In contrast, active Cdc42 levels were not reduced in the $231^{VEGFKOex3}$ cells treated with rhVEGF165 or the bevacizumab-treated 231^{WT} cells, in which the ARHGAP17 level was not altered (Fig. 4*c*).

Cdc42 activity is regulated by multiple GAPs, GEFs and GDIs. However, as shown in Figure 3*c*, only ARHGAP17 was altered by VEGF/NRP1 signaling. Thus, our findings implied that VEGF/NRP1 signaling regulates Cdc42 status via ARHGAP17.

To determine whether regulation of Cdc42 by ARHGAP17 is responsible for morphologic and mobility changes in $231^{VEGFKOex3}$ cells, restoration experiments of ARHGAP17 expression was performed by siARHGAP17. The knock down efficiencies of siARHGAP17 was checked by RT-PCR. The knock down efficiencies of siARHGAP17 oligos were 55, 41 and 59% for siARHGAP17–3, siARHGAP17–5, and both of them, respectively (Supporting Information Fig. S5). The knock down efficiency was also checked by western blotting. Protein level of ARHGAP17 was reduced by both siARHGAP17–3 and siARHGAP17–5 compared to siControl cells (Fig. 4*b*, 0.51-fold). Depending on the knock down efficiency of ARHGAP17, the perimeters and cell migration count of siRNA-treated $231^{VEGFKOex3}$ cells were recovered to the original level of the 231^{WT} cells (Figs. 4*d* and 4*e*).

These findings indicated that ARHGAP17-regulated Cdc42 is responsible for morphologic and mobility change in $231^{VEGFKOex3}$ cells.

VEGF/NRP1/ARHGAP17/Cdc42 network regulates filopodia formation in MDA-MB-231 cells

Cdc42 is crucial for the formation of filopodia, which is important in the motility of cancer cells.[32] Thus, we hypothesized that filopodia formation induced by ARHGAP17/Cdc42 contributed to the VEGF/NRP1-regulated cell migration of MDA-MB-231 cells. We used a scanning electron microscope to observe the filopodia formation of cells. We also counted filopodia number of each cells (Fig. 4*f*). Most of the spreading 231^{WT} cells displayed extended filopodia (Fig. 4*g*), whereas the $231^{VEGFKOex3}$ cells had significantly fewer filopodia (Fig. 4*h*, $p < 0.0001$). In addition, the extension of filopodia was restored by rhVEGF165 treatment to the $231^{VEGFKOex3}$ cells (Fig. 4*i*, $p < 0.0001$). Furthermore, bevacizumab treatment did not show any decrease in filopodia formation (Fig. 4*k*, $p = 0.1521$), whereas sNRP1 overexpression caused decrease of filopodia formation compared to control cells (Figs. 4*m* and 4*n*, $p < 0.0001$). Thus, for the MDA-MB-231 cells, filopodia formation was associated with VEGF signal and Cdc42 activation, and reduction of filopodia formation was correlated with upregulation of ARHGAP17 and inhibition of VEGF.

Taken together, our findings indicate that VEGF/NRP1 signaling regulates cell migration by filopodia formation via ARHGAP17/Cdc42 in MDA-MB-231 cells.

VEGF isoforms differentially regulate ARHGAP17

As shown in Fig. 1*b*, VEGF has various isoforms with different sizes. In experiments above, we used recombinant protein of the most dominant isoform, VEGF165, that contains a neuropilin-binding domain corresponding to exon7-8a. A short isoform, VEGF121, lacks a part of neuropilin binding domain corresponding to exon7, but still has six amino acid tail of exon8a that can bind to NRP1. To determine whether these different VEGF isoforms regulate ARHGAP17 or not, we treated $231^{VEGFKOex3}$ cells with rhVEGF121. As shown in Figures 2*h*, 2*i*, 4*f* and 4*j*, for the 231^{WT} cells, the rhVEGF165 restored cell perimeter, cell migration and filopodia formation to 231^{WT} cell level, whereas rhVEGF121 could not affect it. These results support that interaction between NRP1 and NRP-binding domain of VEGF molecule, corresponding to exon7, is responsible to regulating ARHGAP17, and phenotypic changes of $231^{VEGKOex3}$ cells.

Semaphorin 3A was not regulated by VEGF/NRP1 signal

Semaphorin 3A (SEMA3A) is a member of the semaphorin family that plays a critical role in axonal guidance, and that has recently been recognized as a tumor suppressor.[24,33] SEMA3A and VEGF interact with the b1 domain of NRP1.[34] Thus, SEMA3A can competitively block the binding of VEGF to NRP1. In a previous study, the VEGF/SEMA3A protein ratio was correlated with the cell migration of the BC cell lines.[35] Therefore, *SEMA3A* expression should be monitored concurrently with VEGF expression. In this study, *SEMA3A* mRNA level was upregulated in the $231^{VEGFKOex3}$ cells compared to the 231^{WT} cells (Supporting Information Fig. S6). However, the *SEMA3A* level in the $231^{VEGFKOex3}$ cells was not restored to the original level by the rhVEGF165 treatment. In addition, introduction of exogenous sNRP1 to the 231^{WT} cells did not alter the *SEMA3A* level. Taken together, *SEMA3A* expression was not controlled by VEGF/NRP1 signaling, and

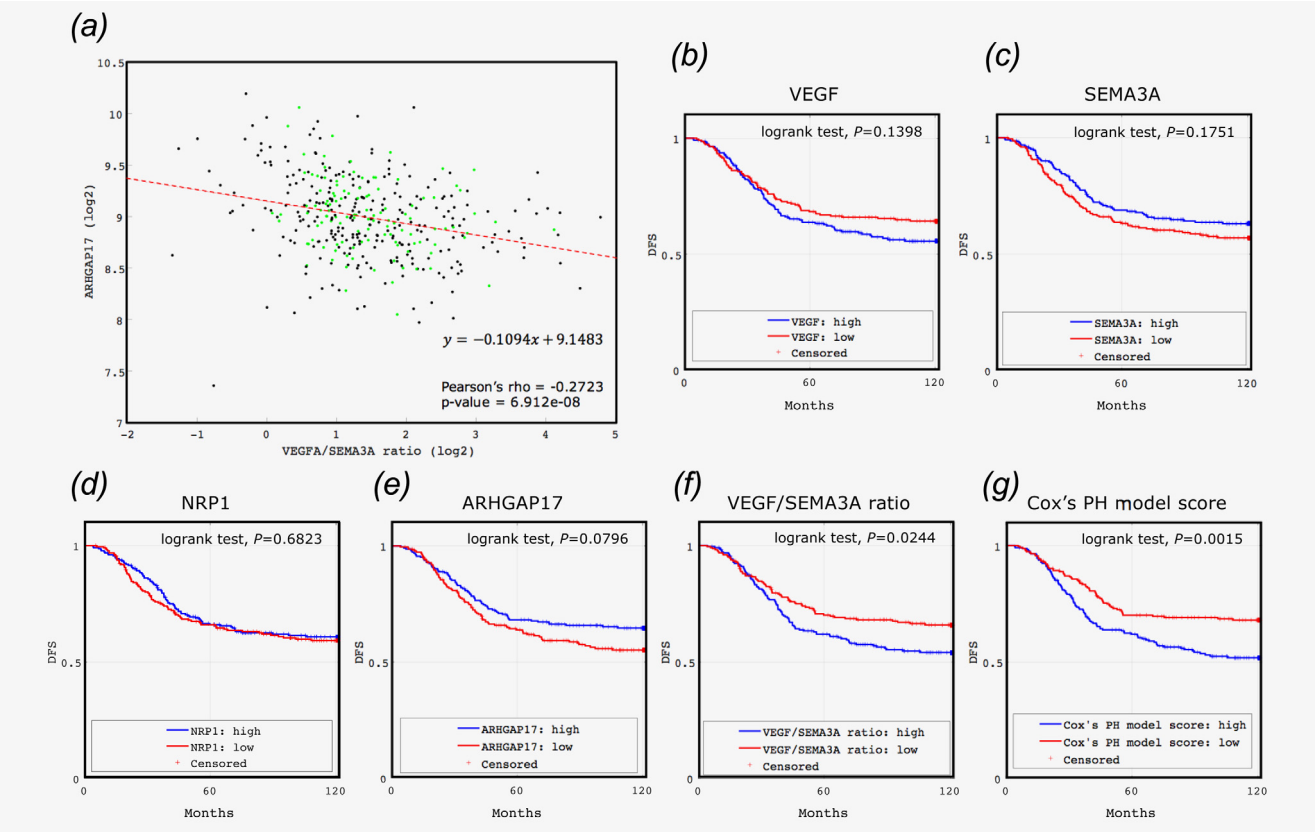

Figure 5. Clinical significance of VEGF/NRP1/ARHGAP17 regulatory network in clinical tissue samples of HR(–) BC. (*a*) Correlation between *VEGFA*/*SEMA3A* ratio and *ARHGAP17* expression in clinical tissue samples. Among 1,980 samples of METABRIC study, 1,468 without copy number alteration at *NRP1* nor *ARHGAP17* locus were selected for this analysis. The *VEGFA*/*SEMA3A* ratio and *ARHGAP17* expression was negatively correlated in pure HER2 and TN subtypes. Black and green dots: TN and pure Her2 subtypes by immunohistochemical four-gene subtyping, red dashed line and equation: regression line and its equation, Pearson's correlation coefficient and its *p*-value are shown. Pearson's and Spearman's correlation coefficients, as well as the *p*-values for each subtype, are listed in Supporting Information Table S6. Impacts of *VEGF* (*b*), *SEMA3A* (*c*), *NRP1* (*d*), *ARHGAP17* (*e*), *VEGF*/*SEMA3A* ratio (*f*), score of Cox proportional hazard model (*g*) on disease free survival of HR(–) BC are represented by Kaplan–Meier curves. *p*: *p*-value of Logrank test. [Color figure can be viewed at wileyonlinelibrary.com]

SEMA3A upregulation in $231^{VEGFKOex3}$ cells was due to a side effect of the CRISPR-Cas9 system.

VEGF/NRP1/ARHGAP17 axis is not an uncommon regulatory network

As above, we demonstrated that MDA-MB-231 cells had a VEGF/NRP1/ARHGAP17 regulatory network. To show generality of our findings, we produced a VEGF-knocked out (exon3) Hs578T breast cancer cells ($578^{VEGFKOex3}$ cells, Supporting Information Fig. S7). The $578^{VEGFKOex3}$ cells exhibited shorter perimeter morphology (Supporting Information Figs. S8*a*–S8*c*) and reduced cell migration ability (Supporting Information Fig. S8*d*). In addition, protein and mRNA expression of ARHGAP17 in $578^{VEFGKOex3}$ cells are upregulated compared to 578^{WT} cells (1.77-fold, Supporting Information Figs. S9*a* and S9*b*). These results are mostly identical to those of $231^{VEGFKOex3}$ cells. Therefore, the VEGF/NRP1/ARHGAP17 axis is not an unusual network.

VEGF/NRP1-dependent regulation of ARHGAP17 in clinical samples

Although the VEGF/NRP1/ARHGAP17/Cdc42 regulatory network works in one TNBC cell line (MDA-MB-231 cell), as demonstrated above, the prevalence of this network in clinical BC tissues remains unknown. To determine whether VEGF signal regulates *ARHGAP17* expression in clinical BC tissue samples, we investigated the relationship between *VEGF* and *ARHGAP17* expression using a publicly available dataset. The dataset of the METABRIC study[36] was downloaded from the cBioportal website,[37] which consisted of clinical information, copy number alteration (CNA) and gene expression data of 1980 primary tumors of BC patients. Among the 1,980 BC samples, 1,468 had no CNA in *NRP1* and *ARHGAP17* gene locus. The expression data of *VEGFA*, *SEMA3A* and *ARHGAP17* genes were extracted from the gene expression dataset. SEMA3A and VEGFA molecules competitively bind to the extracellular domain of NRP1 molecules;[34] thus, distribution of *ARHGAP17* and *VEGFA*/

SEMA3A ratio was shown in a scatter plot, as Supporting Information Figure S10a, and its correlation was estimated by Pearson's and Spearman's methods (Supporting Information Table S6). The samples were stratified into four subtypes according to conventional 3-gene classification (immunohistochemical expression of estrogen receptor, progesterone receptor and HER2). Expression of the *ARHGAP17* and *VEGFA*/*SEMA3A* ratio was negatively correlated in pure HER2-type (n = 117) and TN subtypes (n = 263) with statistically significant p-values (Fig. 5*a*, $p < 0.0001$). In terms of prognosis, among the expression levels of *VEGF*, *SEMA3A*, *NRP1* and *ARHGAP17*, the *VEGF*/*SEMA3A* expression ratio in the primary tumors of HR(−) BC significantly and inversely correlated with disease free survival (DFS) (logrank: p-value = 0.0244, Figs. 5*b*–5*g*, Supporting Information Table S7). Moreover, *ARHGAP17* also tends to correlate with DFS.

Taken together, these findings suggest that the VEGF/NRP1/ARHGAP17 regulatory network would play a role in HR(−) BC tissues (Fig. 5*e*). Furthermore, scores of Cox's proportional hazard model using *VEGF*/*SEMA3A* ratio and *ARHGAP17* predict the DFS of patients efficiently (Fig. 5*g*). Thus, the *VEGF*/*SEMA3A* ratio and *ARHGAP17* may be prognostic markers for HR(−) BCs.

Discussion

VEGF is secreted from a variety of cells in the tumor microenvironment, and plays key roles in tumor angiogenesis in collaboration with its receptors.[5] Bevacizumab is a monoclonal antibody against VEGF that inhibits tumor angiogenesis and growth by blocking VEGF–VEGFR binding on endothelial cells, which is commonly used for the treatment of metastatic BC. To date, accumulating evidence has shown that VEGF is a multifunction molecule that affects a variety of cells in the tumor microenvironment, not only in endothelial cells.[5] Thus, in the current study, we hypothesized that VEGF has a direct effect on BC cells that contributes to their malignant behavior. At first, in vitro experiments using bevacizumab did not show any phenotypic changes in MDA-MB-231 cells. This negative result would be reasonable because MDA-MB-231 cells do not express VEGFR1/2. To prove our hypothesis, we generated a VEGF-knocked out MDA-MB-231 ($231^{VEGFKOex3}$) cells (Fig. 1). Unlike bevacizumab-treated MDA-MB-231 cells, $231^{VEGFKOex3}$ cells displayed morphologic and mobility changes (Fig. 2). Thus, we focused on NRP1 as another VEGF receptor.

The NRP1 consists of a large extracellular domain, one transmembrane domain and a relatively short cytoplasmic tail. In cases where VEGFR is expressed on the cell surface like endothelial cells, a VEGF dimer binds to the VEGFR/NRP1 complex. In such case, NRP1 acts as co-receptor, and the VEGF signal is introduced into cells through the cytoplasmic region of VEGFR. In the present study, we demonstrated that interaction between VEGF and NRP1 without VEGFR contributes to the phenotypic changes of MDA-MB-231 cells. However, how VEGF–NRP1 binding introduces signal into cells remains unknown. Two possible mechanisms for this are as follows. First, the short cytoplasmic tail of NRP1 does not have any tyrosine kinase domain, but a SEA motif that can bind PDZ domains of intracellular proteins such as GIPC (also known as synectin). GIPC is known to promote endothelial migration by collaborating with syndecan-4,[38] and may be a candidate signal transduction molecule interacting with VEGF-activated NRP1. Another possible mechanism would be modulating the functions of other NRP1-interacting membrane receptors.

We demonstrated a function of the VEGF/NRP1/ARHGAP17 regulatory network in vitro. However, the function of this network in vivo had not yet been clarified. Previous studies showed that treatment using a NRP1 transmembrane domain interfering peptide inhibits the tumor growth and metastasis of xenograft of MDA-MB-231 cells.[39] In addition, knock down of Cdc42-interacting protein-4 (CIP4) inhibited lung metastasis formation but not the tumor growth of MDA-MB-231 cells or HCC1806 cells.[40] These data support our in vitro results.

The significance of the VEGF/NRP1/ARHGAP17 network in clinical samples was evaluated using a publicly available dataset: the METABRIC study. *VEGF* expression in clinical tissue specimens of BC is known to be related to patient outcome.[6] In our analysis using the METABRIC study data (Supporting Information Figs. S10*b*–S10*g*), *VEGF* expression in the HR(+) cases significantly correlated with DFS, whereas *NRP1* and *ARHGAP17* expressions did not. In addition, the prognostic impacts (hazard ratios and p-values) of *VEGF* expression and *VEGF*/*SEMA3A* ratio were almost equal (Supporting Information Figs. 10*b* and 10*f*, Supporting Information Table S7), meaning that *SEMA3A* expression had almost no additional prognostic impact. Thus, VEGF/NRP1 signaling does not contribute to DFS in HR(+) BCs. In contrast, *VEGF* expression did not have significant impact to DFS in HR(−) BCs (Fig. 5, p = 0.1398). However, *ARHGAP17* expression tended to correlate with DFS (p = 0.0796), and the hazard ratio of the *VEGF*/*SEMA3A* ratio for DFS was higher than that of *VEGF* only. These results suggest that ARHGAP17 mediated by VEGF–NRP1 interaction partly contributed to DFS in HR(−) BCs. As shown in Supporting Information Table S10, the association between HR status and bevacizumab treatment efficacy in clinical trials has been inconsistent.[9,41–47] Our findings demonstrated that there are bevacizumab-independent VEGF signals in HR(−) BC tumors. These data suggest that VEGF/NRP1/ARHGAP17 network-related markers could predict the outcomes of bevacizumab-related treatment in HR(−) BC cases, but not in HR(+) cases. A prospective study is required to prove the predictive values of these markers.

In this study, we showed that the knocking out of *VEGF* induced ARHGAP17 expression in MDA-MB-231 cells.

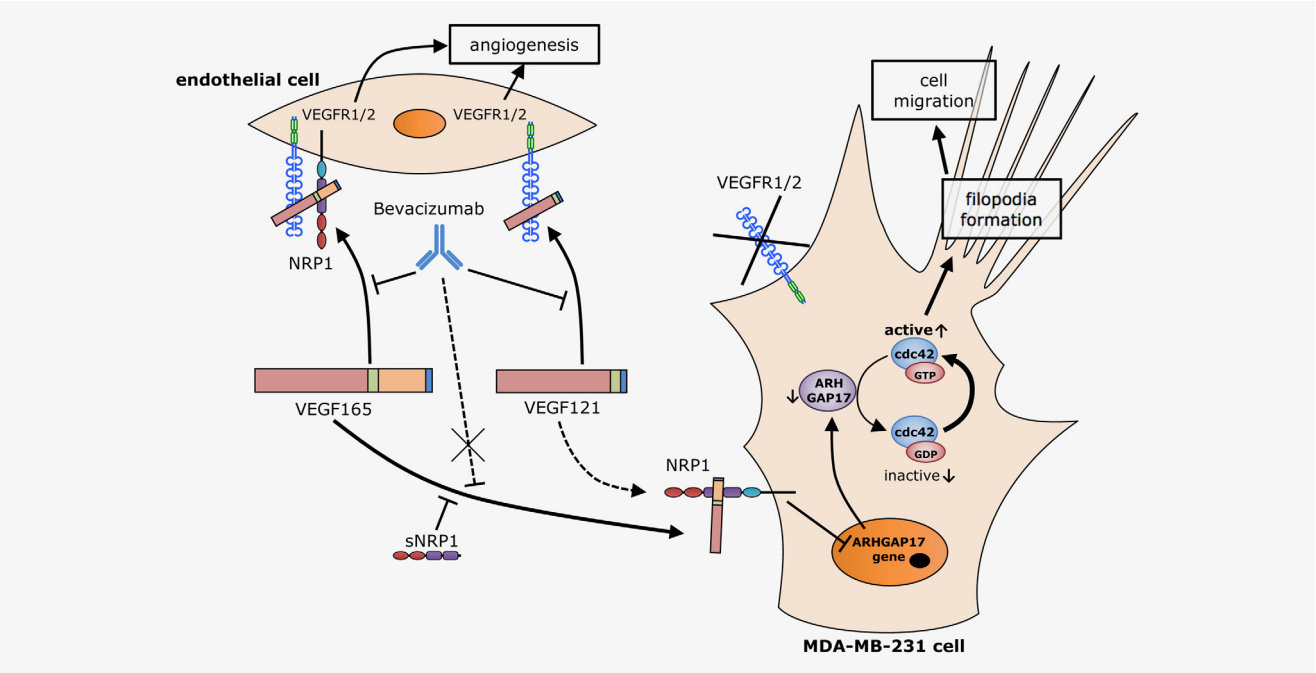

Figure 6. Schematic representation outlining VEGF/NRP1/ARHGAP17/Cdc42 regulatory network in MDA-MB-231 cells. VEGF is secreted from cell members in tumor microenvironment, and acts as a multi-function molecule in autocrine and paracrine fashions. For endothelial cells, both short and long VEGF isoforms (such as VEGF121 and VEGF165) binds to VEGFR1/2 accompanied with NRP1, and promotes angiogenesis. In addition, bevacizumab can inhibit angiogenesis by blocking the interaction between both VEGF isoforms and VEGFR1/2. On the other hand, interaction between NRP1 and long VEGF isoform (VEGF165) but not short VEGF isoform (VEGF121) produces a signal into MDA-MB-231 cells to downregulate ARHGAP17 expression. The downregulation of ARHGAP17 activates Cdc42 status, and increases filopodia formation, resulting in enhanced cell migration ability. Because 231 cells do not express VEGFR1/2, bevacizumab cannot block this VEGF–NRP1 interaction. [Color figure can be viewed at wileyonlinelibrary.com]

Several reports regarding ARHGAP17 focused on its function and interacting molecules.[31,48–52] However, transcriptional regulation of *ARHGAP17* remains unknown. Among BC subtypes, *ARHGAP17* expression in HR(−) tumors is significantly higher than that in HR(+) tumors, according to the METABRIC dataset (Supporting Information Fig. S11). CNA in *ARHGAP17* locus is relatively frequent for HR(+) BC but not for HR(−). Amplification in the *ARHGAP17* locus was present in 26% of HR(+) BCs, but in just 2.6% of HR(−) cases (Chi-square test: $p < 0.0001$). In both the HR(−) and HR(+) tumors, the CNA status of the ARHGAP17 locus clearly correlated with *ARHGAP17* expression. Thus, CNA is one of mechanisms that regulate *ARHGAP17* expression, especially for HR(+) tumors. In terms of epigenetics, there is a CpG island extending from exon1 to intron1 of the *ARHGAP17* gene. According to our previous methylation data of BC cell lines (GSE87177 in GEO database),[53] the CpG island is mostly unmethylated in all BC cell lines. However, one probe at −290 bp from the transcriptional start site of *ARHGAP17* was slightly differentially methylated between luminal (mean beta value: 0.319) and TN BC cell lines (mean beta value: 0.133) (Supporting Information Fig. S12). DNA methylation status around this area in the promoter region might affect transcription of *ARHGAP17* especially for HR(+) tumors. Taken together, *ARHGAP17* expression in HR(+) tumors is regulated by CNA and epigenetics, but CNA and epigenetics are not often involved in HR(−) tumors. Thus, VEGF/NRP1 signal in HR(−) tumors may regulate *ARHGAP17* expression by other mechanisms, such as that which involves transcriptional factors.

To date, efforts have been made to find predictive blood-based biomarkers for bevacizumab treatment outcome, using samples collected in clinical trials. The AVADO trial for mBC[54,55] and the AViTA trial for pancreatic cancer revealed that patients who express high baseline levels of short isoform VEGF exhibit improved progression-free survival and/or overall survival after bevacizumab treatment. These results have been explained as follows; an improved ELISA assay (modified IMPACT Elisa) used in these clinical trials could assess plasma VEGF level with greater sensitivity for short VEGF isoforms than the long isoforms. As shorter VEGF isoforms can diffuse over long distances, this assay could present the plasma level of tumor-derived VEGF that would be biologically relevant in the tumor microenvironment. Our results might provide another explanation for the predictive capability of the short VEGF isoform. Longer VEGF isoforms, such as VEGF165, can bind to both VEGFR and NRP1, whereas VEGF121 can bind to VEGFRs but not to NRP1.[23] As shown in the current study, long VEGF isoforms (VEGF165) have

high affinity to NRP1 to produce signals modulating ARHGAP17. However, short VEGF isoforms (VEGF121) could not produce the signals. In short VEGF-dominant tumors, VEGF/VEGFR signaling would be dominant and could be efficiently blocked by bevacizumab. However, because not only VEGF/VEGFR signaling, but also VEGF/NRP1 signaling may work in long VEGF-dominant tumors, VEGF/NRP1 signaling could remain and contribute to malignant phenotypes of BC even during bevacizumab treatment. This might be a reason why bevacizumab treatment seems to yield better results in patients with high levels of short VEGF isoform.

In conclusion, this study demonstrated the existence of a novel VEGF-related regulatory network that is independent from bevacizumab-treatment. In MDA-MB-231 cells, The NRP1 signal produced by long isoform of VEGF reduces ARHGAP17 expression, and activates Cdc42. Then, Cdc42-mediated filopodia formation consequently increases cell migration (Fig. 6). In addition, the inverse correlation between *VEGF* and *ARHGAP17* was relevant in clinical tissues, and the VEGF-ARHGAP17 network correlated with the prognosis of HR(−) BCs. Thus, the VEGF/NRP1/ARHGAP17/Cdc42 network can be a potential mechanism for bevacizumab treatment resistance.

Author Contributions

FS conceived the study, and MK, SS, MT, FS participated in its design and manuscript preparation. MK and ST carried out all wet lab experiments. FS and MK interpreted the data. FS performed bioinformatics and statistical analyses. All authors have read and approved the final manuscript.

Acknowledgments

We thank Keiko Furuta and Haruyasu Kohda of the Medical Research Support Center, Graduate School of Medicine, Kyoto University, for their technical assistance regarding experiments of scanning election microscopy.

References

1. Torre LA, Bray F, Siegel RL, Ferlay J, Lortet-tieulent J, Jemal A. Global cancer statistics, 2012. *CA Cancer J Clin [Internet]* 2015;65:87–108. Available from: http://onlinelibrary.wiley.com/doi/10.3322/caac.21262/abstract
2. Gierach GL, Burke A, Anderson WF. Epidemiology of triple negative breast cancers. *Breast Dis [Internet]* 2010;32:5–24. Available from: http://www.nature.com/doifinder/10.1038/sj.bjc.6604174%5Cn; http://www.medra.org/servlet/aliasResolver?alias=iospress&doi=10.3233/BD-2010-0319%5Cn; http://www.ncbi.nlm.nih.gov/pubmed/21965309
3. Weigelt B, Peterse JL, van 't Veer LJ. Breast cancer metastasis: markers and models. *Nat Rev Cancer* 2005;5:591–602.
4. Wan L, Pantel K, Kang Y. Tumor metastasis: moving new biological insights into the clinic. *Nat Med [Internet]* 2013;19:1450–64. Available from: http://www.nature.com.proxy.library.adelaide.edu.au/nm/journal/v19/n11/full/nm.3391.html
5. Goel HL, Mercurio AM. VEGF targets the tumour cell. *Nat Rev Cancer [Internet]* 2013;13:871–2. Available from: https://doi.org/10.1038/nrc3627
6. Gasparini G, Toi M, Gion M, et al. Prognostic significance of vascular endothelial growth factor protein in node-negative breast carcinoma. *J Natl Cancer Inst* 1997;89:139–47.
7. Schneider BP, Wang M, Radovich M, et al. Association of vascular endothelial growth factor and vascular endothelial growth factor receptor-2 genetic polymorphisms with outcome in a trial of paclitaxel compared with paclitaxel plus bevacizumab in advanced breast cancer: ECOG 2100. *J Clin Oncol* 2008;26:4672–8.
8. Miles DW, Chan A, Dirix LY, et al. Phase III study of bevacizumab plus docetaxel compared with placebo plus docetaxel for the first-line treatment of human epidermal growth factor receptor 2-negative metastatic breast cancer. *J Clin Oncol* 2010;28:3239–47.
9. Robert NJ, Diéras V, Glaspy J, et al. RIBBON-1: randomized, double-blind, placebo-controlled, phase III trial of chemotherapy with or without bevacizumab for first-line treatment of human epidermal growth factor receptor 2-negative, locally recurrent or metastatic breast cancer. *J Clin Oncol* 2011;29:1252–60.
10. Orimo A, Gupta PB, Sgroi DC, et al. Stromal fibroblasts present in invasive human breast carcinomas promote tumor growth and angiogenesis through elevated SDF-1/CXCL12 secretion. *Cell* 2005;121:335–48.
11. Casanovas O, Hicklin DJ, Bergers G, et al. Drug resistance by evasion of antiangiogenic targeting of VEGF signaling in late-stage pancreatic islet tumors. *Cancer Cell* 2005;8:299–309.
12. Crawford Y, Kasman I, Yu L, et al. PDGF-C mediates the angiogenic and tumorigenic properties of fibroblasts associated with tumors refractory to anti-VEGF treatment. *Cancer Cell* 2009;15:21–34.
13. Leite De Oliveira R, Hamm A, Mazzone M. Growing tumor vessels: more than one way to skin a cat - Implications for angiogenesis targeted cancer therapies. *Mol Aspects Med* 2011;32:71–87.
14. Lyden D, Hattori K, Dias S, et al. Impaired recruitment of bone-marrow-derived endothelial and hematopoietic precursor cells blocks tumor angiogenesis and growth. *Nat Med* 2001;7:1194–201.
15. Shojaei F, Wu X, Malik AK, et al. Tumor refractoriness to anti-VEGF treatment is mediated by CD11b+Gr1+ myeloid cells. *Nat Biotechnol* 2007;25:911–20.
16. Henze A-T, Mazzone M. The impact of hypoxia on tumor-associated macrophages. *J Clin Invest [Internet]* 2016;126:3672–9. Available from: https://www.ncbi.nlm.nih.gov/pubmed/27482883
17. Pàez-Ribes M, Allen E, Hudock J, et al. antiangiogenic therapy elicits malignant progression of tumors to increased local invasion and distant metastasis. *Cancer Cell* 2009;15:220–31.
18. Keith B, Simon MC. hypoxia-inducible factors, stem cells, and cancer. *Cell* 2007;129:465–72.
19. Staton CA, Koay I, Wu JM, et al. Neuropilin-1 and neuropilin-2 expression in the adenoma-carcinoma sequence of colorectal cancer. *Histopathology* 2013;62:908–15.
20. Boro A, Arlt MJE, Lengnick H, et al. Prognostic value and in vitro biological relevance of Neuropilin 1 and Neuropilin 2 in osteosarcoma. *Am J Transl Res* 2015;7:640–53.
21. Kawakami T, Tokunaga T, Hatanaka H, et al. Neuropilin 1 and neuropilin 2 co-expression is significantly correlated with increased vascularity and poor prognosis in nonsmall cell lung carcinoma. *Cancer* 2002;95:2196–1.
22. Fakhari M, Pullirsch D, Abraham D, et al. Selective upregulation of vascular endothelial growth factor receptors neuropilin-1 and -2 in human neuroblastoma. *Cancer* 2002;94:258–63.
23. Koch S. Neuropilin signalling in angiogenesis. *Biochem Soc Trans [Internet]* 2012;40:20–5. Available from: http://www.biochemsoctrans.org/content/40/1/20.abstract
24. Mishra R, Thorat D, Soundararajan G, Pradhan SJ, Chakraborty G, Lohite K, Karnik S, Kundu GC. Semaphorin 3A upregulates FOXO 3a-dependent MelCAM expression leading to attenuation of breast tumor growth and angiogenesis. *Oncogene [Internet]* 2014;34:1584–95. Available from: http://www.ncbi.nlm.nih.gov/pubmed/24727891
25. Oliver AW, He X, Borthwick K, et al. The HPV16 E6 binding protein Tip-1 interacts with ARHGEF16, which activates Cdc42. *Br J Cancer* 2011;104:324–1.
26. Harper SJ, Bates DO. VEGF-A splicing: the key to anti-angiogenic therapeutics? *Nat Rev Cancer [Internet]* 2008;8:880–7. Available from: http://www.pubmedcentral.nih.gov/articlerender.fcgi?artid=2613352&tool=pmcentrez&rendertype=abstract
27. Geretti E, Van Meeteren LA, Shimizu A, et al. A mutated soluble neuropilin-2 b domain antagonizes vascular endothelial growth factor bioactivity and inhibits tumor progression. *Mol Cancer Res* 2010;8:1063–74.

28. Gagnon ML, Bielenberg DR, Gechtman Z, Miao HQ, Takashima S, Soker S, Klagsbrun M. Identification of a natural soluble neuropilin-1 that binds vascular endothelial growth factor: in vivo expression and antitumor activity. *Proc Natl Acad Sci U S A [Internet]* 2000;97:2573–8. Available from: http://www.pubmedcentral.nih.gov/articlerender.fcgi?artid=15970&tool=pmcentrez&rendertype=abstract
29. Huang DW, Sherman BT, Lempicki RA. Systematic and integrative analysis of large gene lists using DAVID bioinformatics resources. *Nat Protoc* 2009;4:44–57.
30. NIH. DAVID bioinformatics resources 6.8 [Internet]. Available from: https://david.ncifcrf.gov
31. Wells CD, Fawcett JP, Traweger A, et al. A rich1/amot complex regulates the cdc42 gtpase and apical-polarity proteins in epithelial cells. *Cell* 2006;125:535–48.
32. Zins K, Gunawardhana S, Lucas T, et al. Targeting Cdc42 with the small molecule drug AZA197 suppresses primary colon cancer growth and prolongs survival in a preclinical mouse xenograft model by downregulation of PAK1 activity. *J Transl Med* 2013;11:1–16.
33. Pan H, Wanami LS, Dissanayake TR, et al. Autocrine semaphorin3A stimulates alpha2 beta1 integrin expression/function in breast tumor cells. *Breast Cancer Res Treat* 2009;118:197–205.
34. Perrot-applanat M, Di Benedetto M. Autocrine functions of VEGF in breast tumor cells: adhesion, survival, migration and invasion. *Cell Adh Migr* 2012;6:547–3.
35. Bachelder RE, Crago A, Chung J, et al. Advances in brief vascular endothelial growth factor is an autocrine survival factor for neuropilin-expressing breast carcinoma cells 1. *Cancer Res* 2001;61:5736–40.
36. Pereira B, Chin S-F, Rueda OM, Vollan H-KM, Provenzano E, Bardwell HA, Pugh M, Jones L, Russell R, Sammut S-J, Tsui DWY, Liu B, et al. The somatic mutation profiles of 2,433 breast cancers refines their genomic and transcriptomic landscapes. *Nat Commun [Internet]* 2016;7:11479. Available from: http://www.nature.com/doifinder/10.1038/ncomms11479
37. cBioPortal for Cancer Genomics [Internet]. Available from: http://www.cbioportal.org/study?id=brca_metabric#summary
38. Tkachenko E, Elfenbein A, Tirziu D, et al. Syndecan-4 clustering induces cell migration in a PDZ-dependent manner. *Circ Res* 2006;98:1398–404.
39. Arpel A, Gamper C, Spenlé C, et al. Inhibition of primary breast tumor growth and metastasis using a neuropilin-1 transmembrane domain interfering peptide. *Oncotarget* 2016;7:54723–32.
40. Cerqueira OLD, Truesdell P, Baldassarre T, Vilella-Arias SA, Watt K, Meens J, Chander H, Osório CAB, Soares FA, Reis EM, Craig AWB. CIP4 promotes metastasis in triple-negative breast cancer and is associated with poor patient prognosis. *Oncotarget [Internet]* 2015;6:9397–408. Available from: http://www.ncbi.nlm.nih.gov/pubmed/25823823%5Cn; http://www.pubmedcentral.nih.gov/articlerender.fcgi?artid=PMC4496225
41. Pivot X, Schneeweiss A, Verma S, et al. Efficacy and safety of bevacizumab in combination with docetaxel for the first-line treatment of elderly patients with locally recurrent or metastatic breast cancer: results from AVADO. *Eur J Cancer* 2011;47:2387–95.
42. Bear HD, Tang G, Rastogi P, Geyer Jr. CE, Robidoux A, Atkins JN, Baez-Diaz L, Brufsky AM, Mehta RS, Fehrenbacher L, Young JA, Senecal FM, et al. Bevacizumab added to neoadjuvant chemotherapy for breast cancer. *N Engl J Med [Internet]* 2012;366:310–20. Available from: http://www.ncbi.nlm.nih.gov/pubmed/22276821
43. von Minckwitz G, Eidtmann H, Rezai M, et al. Neoadjuvant chemotherapy and bevacizumab for HER2-negative breast cancer. *N Engl J Med* 2012;366:299–309.
44. Gianni L, Romieu GH, Lichinitser M, et al. AVEREL: a randomized phase III Trial evaluating bevacizumab in combination with docetaxel and trastuzumab as first-line therapy for HER2-positive locally recurrent/metastatic breast cancer. *J Clin Oncol* 2013;31:1719–25.
45. von Minckwitz G, Puglisi F, Cortes J, Vrdoljak E, Marschner N, Zielinski C, Villanueva C, Romieu G, Lang I, Ciruelos E, De Laurentiis M, Veyret C, et al. Bevacizumab plus chemotherapy versus chemotherapy alone as second-line treatment for patients with HER2-negative locally recurrent or metastatic breast cancer after first-line treatment with bevacizumab plus chemotherapy (TANIA): an open-label, randomised. *Lancet Oncol [Internet]* 2014;15:1269–78. Available from: http://www.sciencedirect.com/science/article/pii/S1470204514704395
46. Bear HD, Tang G, Rastogi P, et al. Neoadjuvant plus adjuvant bevacizumab in early breast cancer (NSABP B-40 [NRG Oncology]): secondary outcomes of a phase 3, randomised controlled trial. *Lancet Oncol* 2015;16:1037–48.
47. Earl HM, Hiller L, Dunn JA, Blenkinsop C, Grybowicz L, Vallier AL, Abraham J, Thomas J, Provenzano E, Hughes-Davies L, Gounaris I, McAdam K, Chan S, Ahmad R, Hickish T, Houston S, Rea D, Bartlett J, Caldas C, Cameron DA, Hayward L, ARTemis Investigators. Efficacy of neoadjuvant bevacizumab added to docetaxel followed by fluorouracil, epirubicin, and cyclophosphamide, for women with HER2-negative early breast cancer (ARTemis): an open-label, randomised, phase 3 trial. *Lancet Oncol [Internet]* 2015;16:656–6. Available from: https://doi.org/10.1016/S1470-2045(15)70137-3
48. Kobayashi Y, Harada A, Furuta B, et al. The role of NADRIN , a Rho GTPase-activating protein , in the morphological differentiation of astrocytes. *J Biochem* 2013;153:389–98.
49. Beck S, Fotinos A, Gawaz M, Elvers M. Nadrin GAP activity is isoform- and target-speci fi c regulated by tyrosine phosphorylation. *Cell Signal [Internet]* 2014;26:1975–84. Available from: https://doi.org/10.1016/j.cellsig.2014.03.024
50. Zhang J, Wang J, Zhou Y, Ren X, Lin M, Zhang Q, Wang Y, Li X. Rich1 negatively regulates the epithelial cell cycle , proliferation and adhesion by CDC42 / RAC1-PAK1-Erk1 / 2 pathway. *Cell Signal [Internet]* 2015;27:1703–2. Available from: https://doi.org/10.1016/j.cellsig.2015.05.009
51. Lee S, Kim H, Kim K, et al. Arhgap17 , a RhoGTPase activating protein , regulates mucosal and epithelial barrier function in the mouse colon. *Sci Rep [Internet]* 2016;6:26923. Available from:. https://doi.org/10.1038/srep26923.
52. Nagy Z, Wynne K, Gambaryan S, et al. cyclic nucleotide-dependent protein kinases target ARHGAP17 and ARHGEF6 complexes in platelets *. *J Biol Chem* 2015;290:29974–83.
53. Uehiro N, Sato F, Pu F, Tanaka S, Kawashima M, Kawaguchi K, Sugimoto M, Saji S, Toi M. Circulating cell-free DNA-based epigenetic assay can detect early breast cancer. *Breast Cancer Res [Internet]* 2016;18:129. Available from: http://breast-cancer-research.biomedcentral.com/articles/10.1186/s13058-016-0788-z
54. Miles DW, De Haas SL, Dirix LY, et al. Biomarker results from the AVADO phase 3 trial of first-line bevacizumab plus docetaxel for HER2-negative metastatic breast cancer. *Br J Cancer* 2013;108:1052–60.
55. Lambrechts D, Lenz H, De Haas S, et al. markers of response for the antiangiogenic agent bevacizumab. *J Clin Oncol* 2013;31:1219–30.